Positive pion production by 149–166 MeV protons on ^{16}O and ^{28}Si

T. P. Sjoreen,* P. H. Pile,† R. D. Bent, M. C. Green, J. J. Kehayias, R. E. Pollock, F. Soga,‡ M. C. Tsangarides,§ and J. G. Wills
Indiana University Cyclotron Facility, Bloomington, Indiana 47405
(Received 18 June 1981)

Angular distributions of the differential cross sections for the reactions $^{16}O(p,\pi^+)^{17}O$(g.s., 0.87 MeV) and $^{28}Si(p,\pi^+)^{29}Si$(g.s., 1.27, 2.03, 3.07, 3.62 MeV) have been measured at several bombarding energies corresponding to pion center-of-mass energies from 7.2 to 21 MeV. In addition, cross section upper limits were obtained at several angles for transitions to the 2.43 and 4.08 MeV states of ^{29}Si at $T_p = 149$ MeV. The systematics of the data are discussed and compared with distorted-wave Born approximation stripping model calculations.

[NUCLEAR REACTIONS ^{16}O, $^{28}Si(p,\pi^+)$, $E_p = 149-166$ MeV; measured $d\sigma/d\Omega(\theta)$, $\theta = 25-155°$; comparison with DWBA stripping model calculations.]

I. INTRODUCTION

The proton-induced nuclear pion production reaction $A(p,\pi)A+1$ leading to discrete bound states in the residual nucleus has several interesting facets. Since near threshold most of the proton kinetic energy is used to create the pion, the reaction involves a high momentum transfer to the residual nucleus. Typical momentum transfers near threshold ($m_\pi c^2 <$ proton kinetic energy <200 MeV) are about twice the average nuclear Fermi momentum ($\cong 270$ MeV/c). Consequently, it is to be hoped that the reaction might provide (once the reaction mechanism is well understood) useful information on the high momentum components of nuclear wave functions. In addition, the reaction process itself is of interest because it produces, as a free particle, one of the constituents of the nuclear force field and is expected to shed light on our understanding of pion-nucleus dynamics. As a result of these hopes and expectations, considerable experimental and theoretical effort has been directed toward understanding the $A(p,\pi)A+1$ process. Recent reviews of pion production have been made by Hoistad,[1] Measday and Miller,[2] and Fearing.[3]

Several different theoretical approaches have been tried to explain existing (p,π^+) data.[1–3] The successes achieved have been qualitative at best and usually apply to a single final state at a single energy. Additional systematic studies of the energy and state dependence of the reaction should provide useful constraints on the theories and help in distinguishing among the various models. To this end, we have studied the energy dependence of the (p,π^+) reaction on targets of ^{16}O and ^{28}Si leading to final states involving the $1d_{5/2}$ and $2s_{1/2}$ orbitals in ^{17}O and the $2s_{1/2}$, $1d_{3/2}$, $1d_{5/2}$, and $1f_{7/2}$ orbitals in ^{29}Si.

The present measurements were carried out at the Indiana University Cyclotron Facility (IUCF) using protons ranging in energy from 149 to 166 MeV. The pions were detected with either a quadrupole-dipole-dipole-multipole (QDDM) spectrometer[4,5] or an opposing dipole ($D\bar{D}$) spectrometer.[6] The experimental procedures employed in the present work are described in Sec. II. More details about the spectrometers are given in Refs. 4–6. The results of the present measurements on the angular distributions of the differential cross section are given in Sec. III. In Sec. IV, the results are compared with previous energy dependence studies,[7,8] and certain systematic features of the data are discussed. Finally, the results are compared with predictions of a DWBA pionic stripping model.[9] Preliminary results of the present measurements have been reported previously.[10]

II. EXPERIMENTAL PROCEDURES

The $^{16}O(p,\pi^+)^{17}O$ measurements were made using baked lithium hydroxide (LiOH) targets with

thicknesses ranging from 34 to 154 mg/cm^2. For the ^{28}Si$(p,\pi^+)^{29}$Si measurements, natural Si targets (92% ^{28}Si) from 12 to 152 mg/cm^2 thick were used. The uncertainties in target thicknesses are $\pm 6\%$.

The present experiments required the use of two different spectrometers. The small D$\overline{\text{D}}$ magnetic spectrometer[6] was employed for pion energies ranging from 5 to 13 MeV, and the QDDM magnetic spectrometer[4,5] for pion energies greater than 13 MeV.

The D$\overline{\text{D}}$ spectrometer is a nondispersive double focusing instrument which has an image size compatible with available commercial silicon surface barrier detectors. It has a 3.5 msr maximum solid angle, a flight path of 77 cm, and a large momentum acceptance (1.5:1 using a 100 mm^2 detector). For the present measurements, the detector array was composed of four elements. The first element was a 76 μm Al absorber, which typically reduced count rates in the next element by a factor of 5 with only a moderate reduction in the pion energy ($\sim$280 keV for a 5-MeV pion). The second element was a 250 μm NE102 plastic scintillator, which gave good flight timing relative to the cyclotron rf beam burst and also provided a ΔE signal. The third element was a 5000 μm Si surface barrier detector which was used to stop the pion and determine its energy. The fourth element was a 500 μm Si detector which acted as a veto. The D$\overline{\text{D}}$ spectrometer was used for the ^{16}O$(p,\pi^+)^{17}$O measurements at $T_p = 154$ and 157 MeV and for the ^{28}Si$(p,\pi^+)^{29}$Si measurements at $T_p = 149$ MeV. The pion spectrum obtained at 90° in the laboratory with a natural Si target is shown in Fig. 1. The energy resolution of this spectrum is approximately 280 keV full width at half maximum (FWHM). The main contributions to this value were from the kinematic energy variation of the pions over the 6.5° horizontal acceptance, beam energy spread, energy straggling of the protons and pions in the target, and straggling of the pions in the Al absorber and the scintillator.

The QDDM spectrometer is used primarily for heavy-charged-particle spectroscopy at IUCF and is much larger than necessary for pion experiments. It has a maximum solid angle of 3.5 msr, a momentum range in the focal plane of 3%, and a dispersion of (15 cm)/(% of momentum range). The focal plane is 45 cm long with a 44° orientation with respect to the central ray. The flight path from the target to the last detector is 6.8 m, corresponding to 84% pion decay for 15-MeV pions. The detector array for pion experiments

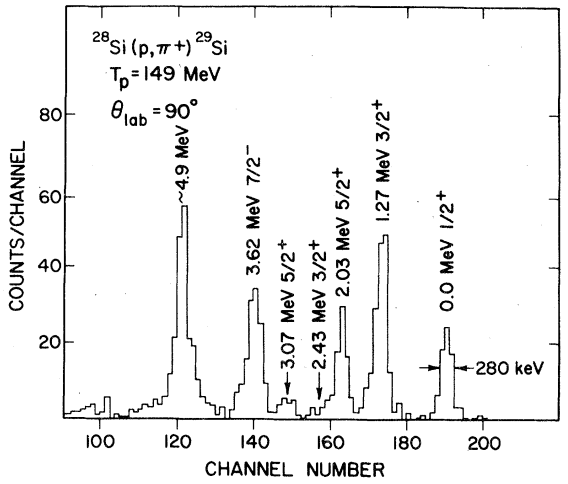

FIG. 1. Pion energy spectrum measured with the D$\overline{\text{D}}$ spectrometer.

consists of a helical multiwire proportional chamber at the position of the spectrograph's horizontal focal plane, followed by 0.32-cm (or 0.64-cm) and 1.27-cm thick scintillators separated by a distance of 30 cm and a third 1.27-cm thick scintillator. The three scintillators were located at the spectrograph's isochronous angle. For low-energy pions which stopped in the second scintillator, the third scintillator was used to veto background due to high-energy protons; for more energetic pions it provided a third ΔE signal. The QDDM spectrometer[4,5] was used to measure pions from the ^{16}O$(p,\pi^+)^{17}$O reaction at 166 MeV and the ^{28}Si$(p,\pi^+)^{29}$Si reaction at 160 MeV. The energy resolution was typically 500–800 keV FWHM and was due primarily to target thickness. Details regarding experimental procedures and data analysis employing the QDDM and D$\overline{\text{D}}$ spectrometers are given in Refs. 4–6, respectively.

III. EXPERIMENTAL RESULTS

The results of the present ^{16}O$(p,\pi^+)^{17}$O and ^{28}Si$(p,\pi^+)^{29}$Si measurements are shown in Fig. 2, where the differential cross sections in the center-of-mass system are plotted as a function of the pion center-of-mass angle. The error bars for the differential cross sections are statistical only. Errors in the absolute cross sections are estimated to be $\pm 15\%$ and $\pm 20\%$ for measurements made with the QDDM and D$\overline{\text{D}}$ spectrometers, respectively.

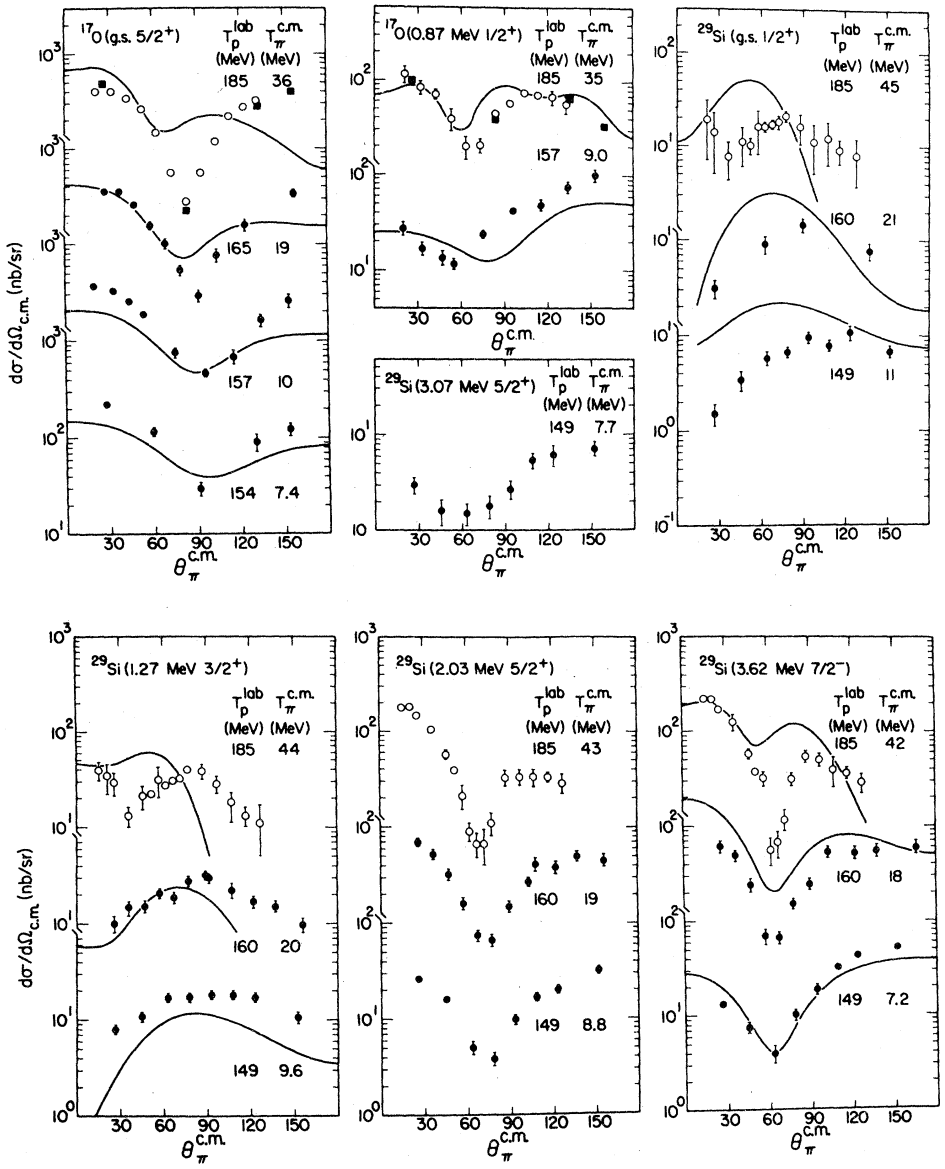

FIG. 2. Angular distribution of the differential cross section for the reactions $^{16}O(p,\pi^+)^{17}O$(g.s. and 0.87 MeV) and $^{28}Si(p,\pi^+)^{29}Si$(g.s., 1.27, 2.03, 3.07, and 3.62 MeV). The present results are denoted by the filled circles, while those denoted by the open circles were taken from Ref. 11. The IUCF data denoted by the squares in the ^{16}O angular distributions were taken at $T_p = 183$ MeV. The curves are the results of DWBA calculations (see text).

The $T_p = 185$ MeV Uppsala[11] differential cross sections are included in Fig. 2. The $^{16}O(p,\pi^+)^{17}O$ and $^{28}Si(p,\pi^+)^{29}Si$ Uppsala cross sections have been multiplied by factors of 1.3 and 1.6, respectively. The 1.3 normalization factor for ^{17}O was determined from the data taken at 183 MeV at IUCF shown in Fig. 2. The 1.6 normalization for ^{29}Si was determined by interpolating between the present results and a 190 MeV $^{28}Si(p,\pi^+)^{29}Si$ measurement at IUCF.[12] The discrepancies among cross sections measured at IUCF, Uppsala, Orsay and TRIUMF are discussed in Ref. 5. The consistency between recent 200 MeV $^{12}C(p,\pi^+)^{13}C$ measurements at IUCF (Ref. 13) and TRIUMF (Ref. 14) supports the present experimental cross sections.

With 280 keV FWHM energy resolution, it was possible with the D$\overline{\text{D}}$ spectrometer to resolve the

ground and 0.87 MeV states in ^{17}O and all the known states below 4.5 MeV in ^{29}Si. However, several of the states were so weakly populated that it was not possible to obtain good statistics with the available beam time. For the ^{17}O ground state, angular distributions were obtained at $T_p = 154$ and 157 MeV with the DD̄, but sufficient statistics to extract a complete distribution for the 0.87 MeV state were taken only at 157 MeV. The larger error bars for the forward angle points of this distribution reflect the difficulty in extracting the peak areas from the tail of the strongly populated ^{17}O ground state. In ^{20}Si, complete angular distributions were obtained for the ground state and the 1.27, 2.03, 3.07, and 3.62 MeV states at $T_p = 149$ MeV. Since the 2.43 and 4.04 MeV states were so weakly populated, it was not possible to extract angular distributions for these states. Based on the present data, it appears that the upper limit for the 2.43 MeV state at $T_p = 149$ MeV is about 2 nb/sr. The 4.08 MeV state has a differential cross section of 10 nb/sr at 25° in the laboratory. The cross section decreases rapidly with increasing angle and is obscured at back angles by the tail of the 3.62 MeV peak.

With the QDDM spectrometer, angular distributions were obtained for the ^{17}O ground state at $T_p = 166$ MeV and the ^{29}Si ground, 1.27, 2.03, and 3.62 MeV states at $T_p = 160$ MeV. Because of the limited energy resolution, the extracted areas for the ^{17}O ground state include some contributions from the 0.87 MeV state, and the ^{29}Si 2.03 and 3.62 MeV peaks also contain pion events from the weaker 2.43, 3.07, and 4.08 MeV states. However, these contributions are believed to be smaller than the statistical errors.

IV. DISCUSSION

The present measurements provide the first energy dependence study of the (p,π^+) reaction to final states in ^{17}O and ^{29}Si. When combined with the 185 MeV Uppsala measurements,[11] the angular distributions cover a range of pion energies from 7 to 36 MeV in ^{17}O and 7 to 45 MeV in ^{29}Si. Angular distributions were obtained for the ^{17}O ground state ($J^\pi = \frac{5}{2}^+$) and the 0.87 MeV ($\frac{1}{2}^+$) excited state, which are known from low energy transfer studies to be good single-particle states involving the $1d_{5/2}$ and $2s_{1/2}$ orbitals, respectively. In ^{29}Si, angular distributions were obtained for the ground state ($\frac{1}{2}^+$) and the 1.27($\frac{3}{2}^+$), 2.03($\frac{5}{2}^+$), 3.07($\frac{3}{2}^+$), and 3.62($\frac{7}{2}^-$) MeV excited states. These states are generally more complicated in structure and typically have small single-particle strengths, except for the 1.27 MeV state, which has a large $1d_{3/2}$ single particle component; the ground, 2.03, and 3.62 MeV states have some particle strength involving the $2s_{1/2}$, $1d_{5/2}$, and $1f_{7/2}$ orbitals, respectively.

The present results, when combined with previous measurements,[7,8] provide comparisons of the energy dependence of the (p,π^+) reaction to final states involving the same orbital for different target masses. An interesting feature which emerges from these comparisons is that the first minimum in the angular distributions for ^{12}C$(p,\pi^+)^{13}$C(3.09, 3.68, and 3.85 MeV (Ref. 8) and ^{16}O$(p,\pi^+)^{17}$O(g.s.) shifts to smaller angles with increasing pion energy, whereas for ^{40}Ca$(p,\pi^+)^{41}$Ca(g.s.) (Ref. 7) there is a pronounced shift in the opposite direction. For ^{29}Si$(p,\pi^+)^{29}$Si(2.03 and 3.62 MeV) there is little shift. On the other hand, the *momentum transfer* at the first minimum in the angular distribution behaves in a more systematic way.

In Fig. 3 the momentum transfer at each minimum ($q_{\min}$) is plotted as a function of the pion momentum (p_π) for the $1f_{7/2}$ final states in ^{41}Ca and ^{29}Si, the $1d_{5/2}$ states in ^{13}C, ^{17}O, and ^{29}Si, and the $2s_{1/2}$ states in ^{13}C, ^{17}O, and ^{29}Si. The ^{41}Ca and ^{13}C results are from Refs. 7 and 8, respectively. The ^{17}O and ^{29}Si data include the Uppsala points.[11] As can be seen from Fig. 3, $q_{\min}$ appears to vary linearly with p_π such that $dq_{\min}/dp_\pi$ is nearly a constant independent of both the final state configuration and the mass of the target. For ^{40}Ca$(p,\pi^+)^{41}$Ca(g.s.), $dq_{\min}/dp_\pi = 0.82 \pm 0.09$.[7] Assuming a linear dependence for the other final states, least squares fits to the data yield values of $dq_{\min}/dp_\pi$ which are consistent with the 0.82 value for ^{41}Ca. A different slope was observed,[8] however, for the 6.86 MeV two-particle one-hole state in ^{13}C; for this case $dq_{\min}/dp_\pi = 1.06 \pm 0.11$.

In addition to the constant value of $dq_{\min}/dp_\pi$, Fig. 3 shows a mass dependence of $q_{\min}$. This is displayed more clearly in Fig. 4, where $q_{\min}$ is plotted by orbitals as a function of the target mass A for an arbitrary pion momentum of $p_\pi = 100$ MeV/c. If $dq_{\min}/dp_\pi$ is a constant, as indicated in Fig. 3, then the relative values of the points in Fig. 4 are independent of the choice of p_π. Figure 4 shows that $q_{\min}$ has a stronger A dependence for transitions to final states involving $2s_{1/2}$ orbitals than for those involving the $1d_{5/2}$ and $1f_{7/2}$ orbitals.

When the dependence of $q_{\min}$ on p_π is taken into account, the angular distributions for transitions

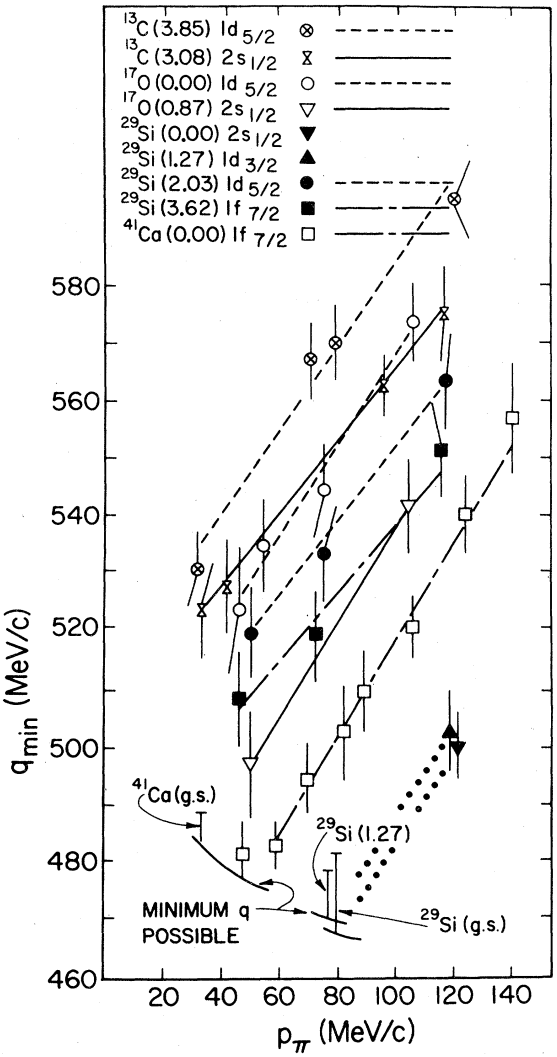

FIG. 3. Momentum transfer at the minima in the angular distributions vs outgoing pion momentum. The carbon and calcium results were taken from Refs. 8 and 7, respectively.

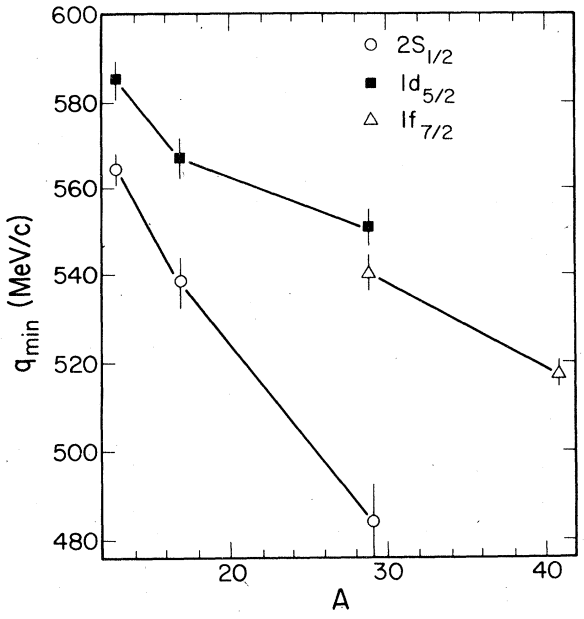

FIG. 4. Momentum transfer at the minima of the angular distributions for $p_\pi = 100$ MeV/c vs target mass for transitions involving different neutron orbitals. The lines are guides for the eye.

between the 0^+ initial states and final states of the same spin and parity are quite similar in shape. This is somewhat surprising, since the ^{29}Si states are more complicated than the relatively pure single particle states in ^{17}O and ^{41}Ca. The similarity is most easily seen in the present data by comparing the ^{17}O ground state and the ^{29}Si 2.03 MeV state angular distributions. The positions of the minima and the magnitude of the cross sections are different, but the shapes of the angular distributions at the same pion energy are remarkably similar. In both cases the target has zero spin and the final state is $\frac{5}{2}^+$; however, the ^{17}O ground state is a good $1d_{5/2}$ single particle state, whereas the ^{29}Si 2.03 MeV state is not (the ^{29}Si state has a very small $1d_{5/2}$ spectroscopic strength[15] of about 0.12). A similar comparison can be made between the angular distributions for the $\frac{7}{2}^-$ ground state in ^{41}Ca (Ref. 7) and the 3.62 MeV state in ^{29}Si. The former is a good $1f_{7/2}$ single particle state, while the latter is a more complex state, which has only a small component of $1f_{7/2}$. In this comparison, however, the ^{41}Ca angular distributions have deeper minima at low pion energies than those for ^{29}Si. Extending the comparison to the states involving the $2s_{1/2}$ orbital is not clear, although some similarities are evident for the ^{17}O 0.87 MeV state, the ^{29}Si ground state, and the ^{13}C 3.08 MeV state.[8] Finally, one interesting comparison can be made between the angular distributions of the $\frac{1}{2}^+$ ground state and the $\frac{3}{2}^+$ 1.27 MeV state in ^{29}Si. Angular momentum and parity considerations require that both reactions involve a transfer of one unit of angular momentum. Comparison of the angular distributions for these two states show that the shape of the distributions are similar at comparable pion energies and that the ratio of the total cross sections are nearly constant with pion energy. The above similarities suggest that the shape of the (p,π^+) angular distributions is determined more by the channel spins and parities and the reaction mechanism than by the details of the nuclear struc-

ture (at least for 0^+ targets).

The curves shown in Fig. 2 are the results of DWBA pionic stripping model calculations.[9] In this model, the pion is emitted by the incident proton and the resulting neutron is captured by the nucleus. A standard, local, optical-model potential with complex central and spin-orbit terms and Woods-Saxon form factors was used to obtain the proton distorted waves. The Coulomb part of this potential was that of a uniform charge distribution. The optical parameters were detemined by proton-nucleus elastic scattering data. The pion distorted waves were calculated by solving a modified Klein-Gordon equation with a local Laplacian pion-nucleus optical potential, which included off-shell damping and corrections for Pauli blocking, true pion absorption, angle transformation, and isoscalar contributions. The shell-model wave functions for the bound-state neutron were calculated employing Woods-Saxon potentials with radius and diffusion parameters constrained to the ranges $r_n = 1.16$ to 1.22 and $a_n = 0.47$ to 0.53 fm, respectively. No attempt was made to determine these parameters from electron scattering data because of the ambiguities involved in determining potentials from nuclear density form factor measurements. Instead, r_n and a_n were varied within the above ranges to obtain best fits to the (p,π^+) data. Other than the values of r_n and a_n and the proton optical model parameters, all of the parameters used in the calculations were taken from Ref. 9.

The calculations for $^{16}O(p,\pi^+)^{17}O$ shown in Fig. 2 were made with $r_n = 1.22$ fm, $a_n = 0.4$ fm, proton optical model parameters taken from Ref. 16, and a spectroscopic factor equal to 1. They reproduce qualitatively the data, indicating that the simple stripping mechanism may contribute significantly to the (p,π^+) process near threshold. Calculations for $^{28}Si(p,\pi^+)^{19}Si$ made with $r_n = 1.2$ fm, $a_n = 0.5$ fm, and proton optical model parameters taken from Ref. 17 are shown for the three states which have the largest single-particle spectroscopic factors (0.53, 0.74, and 0.38 for the 0.0, 1.27, and 3.62 MeV states, respectively[15]). The calculations for the 2.03 MeV states were regarded as unrealistic because of the small (0.12) spectroscopic factor for this state and are not shown. The magnitudes of the calculated cross sections, which are normalized only by the relative spectroscopic factors, are of the same order as the experimental values. The agreement between theory and experiment for the case of $^{28}Si(p,\pi^+)^{29}Si$ is not as good as for $^{16}O(p,\pi^+)^{17}O$, but this is not surprising considering the oversimplified (single-particle) neutron wave functions employed. Somewhat better agreement with the $^{28}Si(p,\pi^+)^{29}Si$(g.s.) data at one energy ($T_p = 185$ MeV) has been achieved in a two-nucleon model calculation.[18]

One problem encountered in trying to optimize the fit between DWBA calculations and the experimental results was the difficulty in getting the minimum in the calculated differential cross section angular distributions to follow the systematic trend $dq_{\min}/dp_\pi = 0.82$ (see Fig. 3). In the plane wave Born approximation $dq_{\min}/dp_\pi = 0$, since the differential cross section is just proportional to the square of the bound neutron wave function in momentum space. By including pion and proton distortions, Tsangarides[9] had only qualitative success in getting the calculated momentum transfer dependence of the minima to agree with experiment.

In summary, several systematic features are observed in the differential cross section data: (1) while the magnitude of the cross sections exhibit a strong state dependence, the shape of the angular distributions appears to be determined primarily by the channel spins and parities and not by details of the nuclear structure; (2) the linear momentum transfer at the first minimum in the angular distributions ($q_{\min}$) for transitions to a particular final state increases approximately linearly with outgoing pion center-of-mass momentum (p_π) such that $dq_{\min}/dp_\pi$ is nearly independent of both the final state and the target mass; and (3) for transitions between the 0^+ initial states and final states of the same spin and parity involving the same neutron orbital, $q_{\min}$ decreases with increasing mass.

The differential cross section measurements presented here, together with those for the reactions $^{12}C(p,\pi^+)^{13}C$(g.s., 3.09, 3.68, 3.85, 6.86, and 9.5 MeV),[8] $^{40}Ca(p,\pi^+)^{41}Ca$(g.s.),[7] and recent polarization asymmetry measurements,[19] constitute a substantial body of information about the energy and state dependence of the (p,π^+) reaction in the near threshold region, which should provide stringent tests of any model of the (p,π) process.

A detailed theoretical interpretation of the simple systematics of the data is currently lacking. Fits to some of the data have been achieved with the DWBA pionic stripping model, but this model does not explain the systematics of the data for a variety of nuclear states, and fails to fit simultaneously differential cross section and analyzing power data.[9] Furthermore, the DWBA approach suffers

from a number of uncertainties (nonrelativistic reduction of the pion production operator, pion-nucleus optical potential, high momentum components of the bound neutron wave function, nonorthogonality of the incident proton, and bound state neutron wave functions) and an undue sensitivity to the input parameters of the model. Only a few two-nucleon model calculations have been made due to their greater complexity. More theoretical work, including detailed comparisons between calculations and the systematics of the data, is needed.

This work was supported in part by the National Science Foundation.

---

*Present address: Oak Ridge National Laboratory, Oak Ridge, Tennessee 37830.

†Present address: Brookhaven National Laboratory, Upton, New York 11973.

‡Present address: Institute for Nuclear Study, University of Tokyo, Tokyo 188, Japan.

§Present address: Scientific Research Labs., Ford Motor Company, Dearborn, Michigan 48121.

[1]B. Höistad, in *Advances in Nuclear Physics,* edited by J. W. Negele and E. W. Vogt (Plenum, New York, 1979), Vol. 11, p. 135.

[2]D. F. Measday and G. A. Miller, Annu. Rev. Nucl. Sci. 29, 121 (1979).

[3]H. W. Fearing, in *Progress in Particle and Nuclear Physics,* edited by D. H. Wilkinson (Pergamon, Oxford, 1981), Vol. 7, p. 113.

[4]R. D. Bent, P. T. Debevec, P. H. Pile, R. E. Pollock, R. E. Marrs, and M. C. Green, Phys. Rev. Lett. 40, 495 (1978).

[5]R. D. Bent, P. H. Pile, R. E. Pollock, and P. T. Debevec, Nucl. Instrum. Methods 180, 397 (1981).

[6]P. H. Pile and R. E. Pollock, Nucl. Instrum. Methods 165, 209 (1979).

[7]P. H. Pile, R. D. Bent, R. E. Pollock, P. T. Debevec, R. E. Marrs, M. C. Green, T. P. Sjoreen, and F. Soga, Phys. Rev. Lett. 42, 1461 (1979).

[8]F. Soga, P. H. Pile, R. D. Bent, M. C. Green, W. W. Jacobs, T. P. Sjoreen, T. E. Ward, and A. G. Drentje, Phys. Rev. C 24, 570 (1981).

[9]M. Tsangarides, Ph.D. thesis, Indiana University, 1979 (unpublished).

[10]T. P. Sjoreen, R. D. Bent, M. C. Green, P. H. Pile, R. E. Pollock, and F. Soga, Bull. Am. Phys. Soc. 24, 614 (1979).

[11]S. Dahlgren, P. Grafström, B. Höistad, and A. Åsberg, Nucl. Phys. A227, 245 (1974).

[12]W. W. Jacobs, A. G. Drentje, P. H. Pile, P. P. Singh, T. P. Sjoreen, and S. E. Vigdor, Phys. Lett. 94B, 319 (1980).

[13]B. Höistad, P. H. Pile, T. P. Sjoreen, R. D. Bent, M. C. Green, and F. Soga, Phys. Lett. 94B, 315 (1980).

[14]E. G. Auld, A. Haynes, R. R. Johnson, G. Jones, T. Masterson, E. L. Mathie, D. Ottewell, P. Walden, and B. Tatischeff, Phys. Rev. Lett. 41, 462 (1978).

[15]M. C. Mermaz, C. A. Whitten, Jr., J. W. Champlin, A. J. Howard, and D. A. Bromley, Phys. Rev. C 4, 1778 (1971).

[16]I. Abdul-Jalil and D. F. Jackson, J. Phys. G 5, 1699 (1979).

[17]A. Nadasen, P. Schwandt, P. P. Singh, W. W. Jacobs, A. D. Bacher, P. T. Debevec, M. D. Kaitchuck, and J. T. Meek, Phys. Rev. C 23, 1023 (1981).

[18]M. Dillig and M. G. Huber, Phys. Lett. 69B, 429 (1977).

[19]T. P. Sjoreen, P. H. Pile, R. E. Pollock, W. W. Jacobs, H. O. Meyer, R. D. Bent, M. C. Green, and F. Soga, Phys. Rev. C 24, 1135 (1981).